Journal of Luminescence, 2003, 101 (3) : 167-174.
http://dx.doi.org/10.1016/S0022-2313(02)00410-6

The Luminescence of Sm^{2+} in Alkaline Earth Borophosphates

Qinghua Zeng, Nathan Kilah and Mark Riley

Abstract

The temperature-dependent luminescence of Sm^{2+} ions in $MBPO_5$ (M=Ca^{2+}, Sr^{2+}, Ba^{2+}) was studied. At low temperature, Sm^{2+} in this series shows $4f^6 \rightarrow 4f^6$ luminescence with only a single emission line observed for the $^5D_0 \rightarrow {}^7F_0$ transition, revealing that only one crystallographic cationic site is available for Sm^{2+} in all the hosts. With increasing temperature, the emission intensity of the $^5D_0 \rightarrow {}^7F_0$ transition increases whereas that of the $^5D_0 \rightarrow {}^7F_1$ transitions decreases. The $^5D_1 \rightarrow {}^7F_0$ transitions of Sm^{2+} were observed in $BaBPO_5$ and its intensity increases with increasing temperature. At 450 K, a broad band of the $4f^55d \rightarrow 4f^6$ luminescent transition of Sm^{2+} in $SrBPO_5$ and $BaBPO_5$ with maximum at ~600 nm appears due to the thermal population. The lifetime of the $^5D_0 \rightarrow {}^7F_0$ transition was recorded at different temperatures, showing a single exponential decay for Sm^{2+} in $SrBPO_5$ and $BaBPO_5$ but a non-single-exponential decay in $CaBPO_5$.

Keywords: Samarium(II); $CaBPO_5$; $SrBPO_5$; $BaBPO_5$

PACS classification codes: 78.55.−m; 78.20.−e; 42.62.Fi

1. Introduction

The spectral hole burning (SHB) in rare-earth-doped materials have attracted considerable interest due to its potential for use in optical data storage in high-density memory devices. Sm^{2+}-doped inorganic materials are quite attractive since spectral holes can show relatively high thermal stability [1 and 2]. The hole burning of Sm^{2+} in single crystals of SrB_4O_7 was recently reported [3]. This is a new system for spectral hole burning of Sm^{2+} as most of the previous research was concentrated on the halides and borosilicates glasses, where a strong reducing atmosphere or high energy irradiation, for example γ-rays, is required for the reduction of Sm^{3+} to Sm^{2+} [4]. For crystalline and polycrystalline SrB_4O_7, the valence change from Sm^{3+} to Sm^{2+} can be easily achieved in air and the Sm^{2+} ion shows highly efficient luminescence at room temperature [3, 5 and 6]. The ease of incorporation and stabilization of Sm^{2+} in this material is because of its unique structure. In SrB_4O_7, all of the boron atoms are tetrahedrally coordinated forming a three-dimensional $(B_4O_7)_\infty$ network by corner-sharing. The network contains channels parallel to *b*-axis. The strontium ions fit into these channels and are surrounded by nine oxygen ions, giving SrO_9 polyhedral, with C_s symmetry. The divalent rare earth ions are thus located in a "cage" formed by BO_4 units of the $(B_4O_7)_\infty$ framework. Such a framework is thought to be a rigid structure preventing the divalent rare-earth ions from being oxidized [7 and 8].

The crystalline alkaline earth borophosphates $MBPO_5$ (M=Ca^{2+}, Sr^{2+}, Ba^{2+}) were reported to be isostructural with stillwellite-$LnBSiO_5$ (Ln refers to lanthanide), built up by BO_4 and SiO_4 tetrahedra [9]. The SiO_4 tetrahedra form edge-sharing vertical columns parallel to the *c*-axis. Each BO_4 tetrahedron is connected with two SiO_4 tetrahedra and has two common edges with the lanthanide polyhedra of adjacent columns forming helical chains. Lanthanide ions are located in the center of this helix and coordinated with nine oxygens as LnO_9 polyhedral with C_2 symmetry [10, 11, 12 and 13]. This structure also suggests that the hosts $MBPO_5$ should be a good candidate for luminescence for rare-earth ions. The

luminescent efficiency of Eu^{2+} in this series of hosts was reported to be high at low temperature [14]. The phosphor $SrBPO_5:Eu^{2+}$ shows intense luminescence under UV and X-ray radiation and was considered to be a more favorable material as an X-ray storage phosphor than the currently used $BaFBr:Eu^{2+}$. The Stokes shift is only about 2900 cm^{-1} [15], indicating that the relaxation in the excited state is restricted by the host lattice [16]. It seems that these borophosphates are a new system for highly efficient luminescence. To the best of our knowledge, no studies of rare-earth ions other than Eu^{2+} have been performed in $MBPO_5$. In this paper, we report on the temperature-dependent luminescence of Sm^{2+} ions in $MBPO_5$.

2. Experiments

The samples of $MBPO_5$ ($M=Ca^{2+}$, Sr^{2+}, Ba^{2+}) doped with Sm^{2+} were prepared by firing the stoichiometric mixtures of MCO_3 ($M=Ca^{2+}$, Sr^{2+}, Ba^{2+}), H_3BO_3 (3 mol% excess), $(NH_4)_2HPO_4$ (5 mol% excess) and Sm_2O_3 in a muffle furnace under a H_2/He (20% H_2) atmosphere. The concentration of dopant Sm_2O_3 (99.9%) was 2 mol% of the M^{2+} ions. The mixture was first preheated at 600°C for 2 h, then ground and heated at 800°C for further 5 h. The structure was checked by a Bruker Model D8 Advance X-ray powder diffractometer with a SOL-X EDS detector using Co K□ radiation. All the samples appear to be single phase.

The excitation spectra were recorded with a Perkin–Elmer Luminescence Spectrometer Model LB-50B with an 8 W (equivalent 20 kW) pulsed Xenon lamp as an excitation source at room temperature. The lamp output power were corrected for the excitation measurements. The high-resolution emission spectra and decay time were recorded using Ar^+ ion laser excitation at 488 nm with a Spex-1702 0.75 m monochromator with a resolution of about 0.1 nm. The light was detected with an R430-02 cooled photomultiplier tube (PMT) and a Stanford SR400 gated photoncounter. The emission spectra were not corrected for the detector and grating response. For the decay time measurements, an IntraAction AFM-603 Acoustic Optical Modulator controlled by a Stanford Research DS345 Function Generator was used to chop the 488 nm line of the Ar^+ laser. The detected pulses were amplified by a Stanford Research SR445 Amplifier for two stages and recorded on a FastTech P7886 multichannel scaler. A self-made furnace and liquid nitrogen Dewar were used for high- and low-temperature measurements, respectively. The measurements were controlled by LabView software.

3. Results and discussion

Divalent Sm^{2+} has the $4f^6$ electron configuration, which under irradiation with UV and visible light can be excited into the $4f^55d^1$ continuum. The excitation spectra at room temperature of Sm^{2+}-doped $MBPO_5$ are shown in Fig. 1. Sm^{2+} ions in all three hosts show similar excitation features. The excitation spectra roughly consist of two broad bands with two maxima at around 350 and 450 nm, together with some sharp peaks between 250 and 500 nm. These broad bands arise from the $4f^6 \rightarrow 4f^55d^1$ transitions of Sm^{2+} ions. To assign these bands, we have to take into account the crystal field of splitting of $4f^5$ and $5d^1$ levels. In $MBPO_5$, the cationic ions M^{2+} are of nine coordinate as SrO_9 polyhedral on a C_2 site [10, 11, 12 and 13]. As an approximation, Sr^{2+} is considered to locate in a cubic center, namely, eight of the nine coordinating oxygens are roughly on the corner of a cube and the ninth oxygen is on one of the tetragonal axes. In an eight-coordinated cubic center, the 5d level is split into a lower e_g and a higher t_{2g} level by the crystal field. From the difference in the two maxima in the excitation spectrum shown in Fig. 1, the crystal field splitting of 5d electron in these three hosts is ~6500 cm^{-1}, which is similar to that observed previously [17]. The excitation spectrum of Sm^{3+} in $CaBPO_5$ as also shown in Fig. 1 for comparison, and the rather strong sharp peak at 400 nm is shown to correspond to the absorption band of the $^5H_{5/2} \rightarrow {}^4K_{11/2}$ transition in the Sm^{3+} ions present in the sample. The presence of Sm^{3+} ions in the $CaBPO_5$ host is also detected in the emission spectrum (see below).

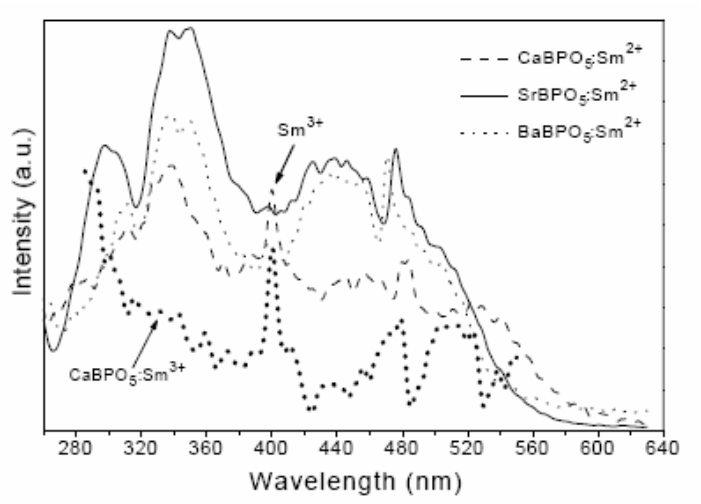

Fig. 1. The excitation spectra of Sm^{2+} in $MBPO_5$ (M=Ca^{2+}, Sr^{2+}, Ba^{2+}) at room temperature, monitoring the $^5D_0 \rightarrow {}^7F_0$ luminescence at ~680 nm. (The dot line is the excitation of Sm^{3+} in $CaBPO_5$ monitoring the $^4G_{5/2} \rightarrow {}^6H_{7/2}$ transitions at 610 nm.)

The emission spectra of Sm^{2+} doped in $MBPO_5$ at 77 K are shown in Fig. 2. Several groups of sharp lines can be observed. No broad emission band was observed at room temperature in any of the samples. The emission of Sm^{2+} in the three hosts show similar features and result from transitions between levels of the $4f^6$ electron configuration. The ground state levels of Sm^{2+} arise from the ^7F_J ($4f^6$) multiplet, where the J=0–6 states occur at successively higher energies. The lowest excited state is $^5D_0$ and therefore, the emission is the result of the $^5D_0 \rightarrow {}^7F_J$ transitions. The assignment and the peak positions of these emission lines are given in Table 1.

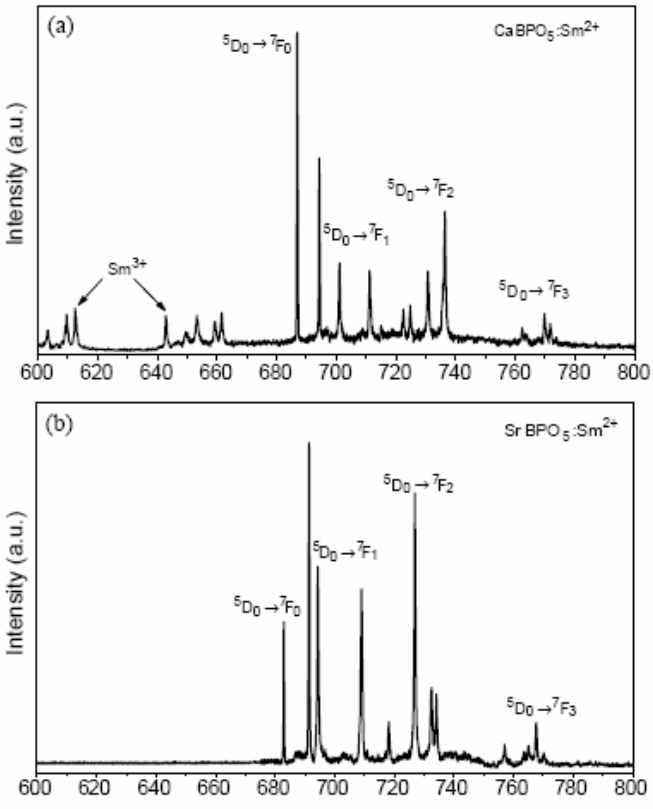

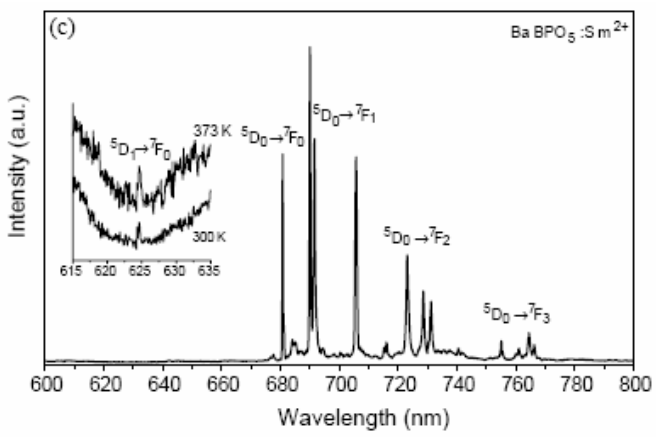

Fig. 2. The emission spectra of Sm^{2+} in $MBPO_5$ (M=Ca^{2+}, Sr^{2+}, Ba^{2+}) at 77 K.

Fig 2a shows the emission spectrum of Sm^{2+} in $CaBPO_5$. Four groups of lines from 680 to 840 nm correspond to the $^5D_0 \rightarrow {}^7F_J$ (J=0,1,2,3) transitions of Sm^{2+} in the host which are split by the crystal field. There is clearly one line for $^5D_0 \rightarrow {}^7F_0$, three for the $^5D_0 \rightarrow {}^7F_1$ and four for the $^5D_0 \rightarrow {}^7F_2$ transitions. The $^5D_0 \rightarrow {}^7F_0$ transition at 686.9 nm has the strongest intensity. The three lines at 694.4, 701.1 and 711.2 nm are attributed to the $^5D_0 \rightarrow {}^7F_1$ transitions, indicating that the degeneracy of the $^7F_1$ level has been completely lifted and these lines are well separated with an overall splitting of about 340 cm^{-1}. The lines from 722.5 to 736.5 nm correspond to the $^5D_0 \rightarrow {}^7F_2$ transitions and those at around 770 nm are assigned to $^5D_0 \rightarrow {}^7F_3$ transitions.

Table 1. The assignment and the peak positions (in nanometers) of the Sm^{2+} $^5D_0$–^7F_J transitions in $MBPO_5$ (M=Ca^{2+}, Sr^{2+}, Ba^{2+}) at 77 K

$^5D_0 \rightarrow {}^7F_J$	$CaBPO_5$: Sm^{2+}	$SrBPO_5$: Sm^{2+}	$BaBPO_5$: Sm^{2+}
$J = 0$	686.9	682.1	681.1
$J = 1$	694.4	690.7	690.5
	701.0	693.5	692.0
	711.1	707.7	705.7
$J = 2$	722.6	717.8	715.9
	724.9	726.0	716.1
	730.9	731.5	723.2
	736.4	733.1	728.8
			731.1

The emission spectrum of Sm^{2+} in $SrBPO_5$ at 77 K is shown in Fig. 2b, the assignments and peak positions are also given in Table 1. Again, there is also one line for $^5D_0 \rightarrow {}^7F_0$, three for $^5D_0 \rightarrow {}^7F_1$ and four for $^5D_0 \rightarrow {}^7F_2$ transitions. However, the integrated intensity of the $^5D_0 \rightarrow {}^7F_0$ transition is weaker than that of $^5D_0 \rightarrow {}^7F_1$ transitions at around 691 nm, which is different from Sm^{2+} in $CaBPO_5$ shown above. The emission spectra of Sm^{2+} in $BaBPO_5$ at 77 K is shown in Fig. 2c. There is one line for the $^5D_0 \rightarrow {}^7F_0$ transition and three for the $^5D_0 \rightarrow {}^7F_1$ transitions. Like in $SrBPO_5$ but unlike in $CaBPO_5$, the dominant line of Sm^{2+} in this host is from the $^5D_0 \rightarrow {}^7F_1$ transitions. There are five lines for $^5D_0 \rightarrow {}^7F_2$ transition which is in agreement with the theoretical splitting of the $^7F_2$ multiplet into a maximum of five sublevels. From Fig. 2 and Fig. 3, it is observed that the position of the $^5D_0$ level shifts towards higher energy in the sequence $CaBPO_5$, $SrBPO_5$ and $BaBPO_5$. This is due to the increasing cation-ligand distance, leading to a decrease of the covalency and nephelauxetic effect [18].

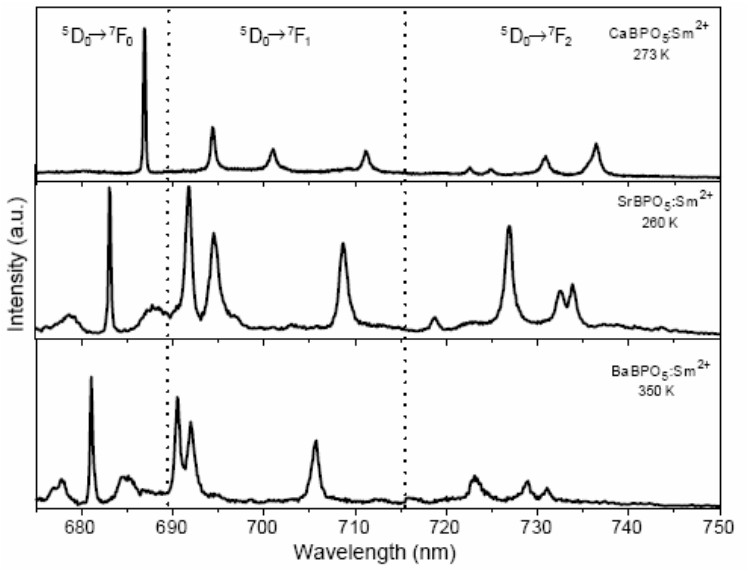

Fig. 3. The emission spectra of Sm^{2+} in $CaBPO_5$ (273 K), $SrBPO_5$ (260 K) and $BaBPO_5$ (350 K).

In addition to the strong emission lines presented in Fig. 2, weaker lines situated at the lower energy side of the $^5D_0 \rightarrow {}^7F_0$, $^5D_0 \rightarrow {}^7F_1$ and $^5D_0 \rightarrow {}^7F_2$ transitions can be observed. These bands are ascribed to the vibronic transitions, resulting from the interactions between the electrons and the lattice during the transitions between these two levels. The energy displacement with zero-phonon line is at ~70 and 100 cm^{-1} in each side which is ascribed to a lattice phonon and its intensities increase with increasing temperature. This result is similar to that seen in the emission of other divalent rare-earth luminescence [19 and 20]. The vibronic transitions are not observed in $CaBPO_5$. In these hosts, only single phonons were coupled with the transitions and sharp vibronic lines appear. In some hosts, the transitions are coupled with all the lattice vibrational mode of the hosts and this results in broader sidebands rather than lines [21].

The very weak peak at around 624.6 nm as shown in the inset in Fig. 2c corresponds to the $^5D_1 \rightarrow {}^7F_0$ transition. Its intensity increases when the temperature is raised, as it results from the $^5D_1$ level being thermally populated from the $^5D_0$ level. The luminescence from the $^5D_1$ level to ^7F_J levels does not occur at low temperature since the energy gap between $^5D_1$ and $^5D_0$ levels is about 1350 cm^{-1}. This is very close to the highest frequency of the asymmetric stretching mode of BO_4 and BO_3 groups [22], leading to a very fast non-radiative relaxation between $^5D_1$ and $^5D_0$ levels. The same phenomena are also observed in other borates doped with Sm^{2+}ions [19 and 20]. The observation of Sm^{2+} $^5D_1 \rightarrow {}^7F_J$ luminescence thus varies greatly between host materials, depending on the energy gap between $^5D_0$ and $^5D_1$ levels, the phonon energy and the energy of the $4f^55d^1$ states. In halides doped with Sm^{2+} ions, for example in BaClF [23], the direct excitation and emission from the $^5D_1$ level was observed at 15 K and it decreases in intensity with increasing temperature, becoming completely quenched at 650 K. In $MBPO_5$ (M=Ca^{2+}, Sr^{2+}, Ba^{2+}), the $^5D_1 \rightarrow {}^7F_0$ transition was observed only in the Ba^{2+} host at the temperatures investigated. Fig. 2 shows that the $^5D_0$ level is located at a relatively higher energy in $BaBPO_5$ than in the Ca^{2+} and Sr^{2+} hosts, it is expected that the $^5D_1$ will also be located at a slightly higher energy in Ba^{2+} borophosphate than in other two hosts. The excitation spectra in Fig. 1 shows that the transition to the $4f^55d^1$ state also increases in the series Ca^{2+}, Sr^{2+}, Ba^{2+}. This increase (~20 nm) is greater than the increase (~5 nm) of the $^5D_0 \rightarrow {}^7F_0$ transition along the Ca^{2+}, Sr^{2+}, Ba^{2+} series. Thus, the energy separation between $4f^55d^1$ and $^5D_1$ level will be larger in Ba^{2+} than in Ca^{2+} and Sr^{2+} hosts. The larger energy separation of the $^5D_1$ and $4f^55d^1$ states may be the reason why the $^5D_1 \rightarrow {}^7F_0$ luminescence is only observed for the Ba^{2+} compound. In the Ca^{2+} and Sr^{2+} hosts, the nearby $4f^55d^1$ states may completely quench the $^5D_1 \rightarrow {}^7F_0$ emission.

In addition of the main emission lines in Fig. 2a in $CaBPO_5$, some other lower intensity lines in the 600–662 nm range can be observed. These lines are due to the $^4G_{5/2} \rightarrow {}^6H_{7/2,9/2}$ transitions within the $4f^5$ configuration of the small amount of Sm^{3+} ions present in the host even though these samples are prepared in a reducing atmosphere. A very small amount Sm^{3+} could also possibly exist in $BaBPO_5$ from its extremely weak fluorescence spectra. No emission from Sm^{3+} ions in $SrBPO_5$ was detected. The relative intensities of these transitions in Ca^{2+} and Ba^{2+} hosts imply that the amount of Sm^{3+} in $CaBPO_5$ is much greater than in $BaBPO_5$. This result is reasonable as the greater the radius mismatch, the more difficult it is to reduce samarium to the divalent state and less stable it becomes. Since the ionic radius of Sm^{2+} ion (146 pm [24]) is similar to that of the Sr^{2+} ion (145 pm) compared with Ca^{2+} (132 pm) and Ba^{2+} (161 pm), it is expected that Sm^{3+} is easier to reduce to the divalent state and is more stable in the Sr^{2+} host. This is especially true in $CaBPO_5$ since the radius of Sm^{3+} (127 pm) is close to that of Ca^{2+} and more samarium ions remain in trivalent state than in the other two hosts.

The temperature dependence on the luminescence of Sm^{2+} in $MBPO_5$ has been measured from 77 to 450 K. The Sm^{2+} ion in all hosts shows strong emission at liquid nitrogen and room temperature. The fluorescence intensity of Sm^{2+} ion in $CaBPO_5$ was strongly temperature dependent, but much less pronounced for $SrBPO_5$ and $BaBPO_5$. As the temperature increases, the emission intensity of Sm^{2+} in $CaBPO_5$ decreases sharply and is completely quenched at around 350 K. In $SrBPO_5$ and $BaBPO_5$, the emission of Sm^{2+} also decreases with increasing temperature. At 373 K, the intensity decreases to 50% of that at room temperature. A similar thermal behavior was also observed in the fluorescence of Eu^{2+} in $MBPO_5$ [14]. The authors reported that the $MBPO_5:Eu^{2+}$ showed high efficiency at low temperature but the luminescence decreases when temperature increased, especially in $CaBPO_5$, where the Eu^{2+} was nearly quenched at room temperature. In all host lattices thermal quenching may result from non-radiation processes. From the excitation spectra shown in Fig. 1, one can find that the lowest $4f^5 5d^1$ level is situated at a relatively lower energy in $CaBPO_5$ than in $SrBPO_5$ and $BaBPO_5$, which may result in a lower quenching temperature. The quenching temperature for Sm^{2+} in $SrBPO_5$ and $BaBPO_5$ are not obtained at the temperatures investigated. At 450 K, the emission spectra of Sm^{2+} in both samples consist of sharp lines and a broad band with a maximum at around 600 nm as shown in Fig. 4. This broad band is assigned to the $4f^5 5d^1 \rightarrow {}^7F_J$ transitions of Sm^{2+} as reported in other borates [20]. For Sm^{2+} in $SrBPO_5$ and $BaBPO_5$, the $4f^5 5d^1$ level is located at slightly higher energy than the $^5D_0$ state.

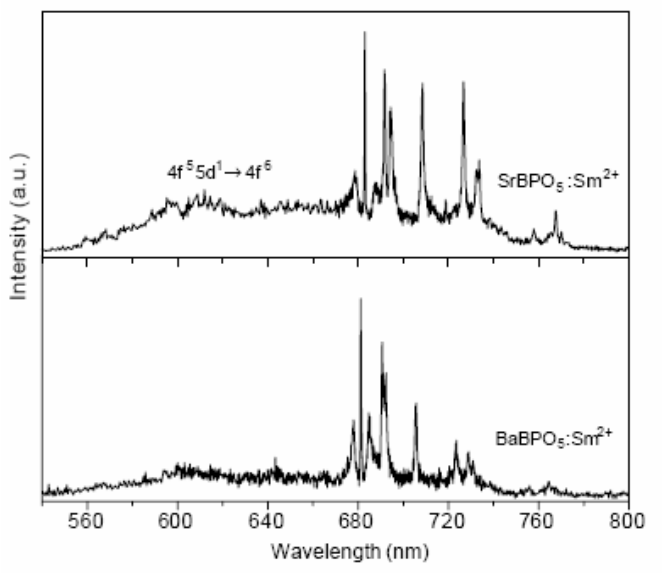

Fig. 4. The emission spectrum of Sm^{2+} in $SrBPO_5$ and $BaBPO_5$ at 450 K.

At low temperature, the excited electrons in $4f^5 5d^1$ level will undergo a non-radiative relaxation to the $^5D_0$ state and give rise to the f–f transitions, while at high temperature the electrons can be thermally pumped to $4f^5 5d^1$ level and lead to a broad emission band. With further increasing temperature, the integrated intensities of all the transitions will be quenched. As for the quenching of the $^5D_1 \rightarrow {}^7F_J$ transitions, the mechanism has been studied in [25] where the authors suggested a so-called "two-step" quenching process of $^5D_1 \rightarrow 5d \rightarrow {}^5D_0$ crossovers. The multi-phonon relaxation between $^5D_0$ and ^7F_J can be neglected at low temperature since the energy gap between these two levels (typically the energy gap between $^5D_0$ and the highest-lying $^7F_6$ level is about 10500 cm^{-1}) is more than nine times larger than the highest lattice vibrations (the BO_4 stretching mode is around 1200 cm^{-1}). As is known, a multiphonon relaxation with more than seven phonons is ineffective [26]. The study of the temperature dependence of the luminescence of Sm^{2+} in these three hosts shows that the temperature variation of Sm^{2+} fluorescence is strongly governed by the lowest lying $4f^5 5d^1$ states. As a result, when describing the temperature dependence of Sm^{2+} fluorescence in a series of similar lattices, the variation of the f–d energy gap must be taken into account.

In $SrBPO_5$ and $BaBPO_5$, the peak heights of the $^5D_0 \rightarrow {}^7F_1$ transitions are higher than that of the $^5D_0 \rightarrow {}^7F_0$ transition below 260 and 310 K, respectively. As the temperature is raised the $^5D_0 \rightarrow {}^7F_1$ peaks tend to decrease faster compared to the $^5D_0 \rightarrow {}^7F_0$ peak, as shown in Fig. 2 and Fig. 3. The relative integrated intensities, however, show much less variation as expected, but it is difficult to quantify as at higher temperature the intensity is redistributed into vibronic bands that tend to contribute to the broad underlying baseline.

The luminescence lifetimes of the Sm^{2+} $^5D_0 \rightarrow {}^7F_0$ transition in $MBPO_5$ were recorded as a function of temperature (Fig. 5). The decay curves are single exponential in $SrBPO_5$ and $BaBPO_5$ at all temperatures. At 77 K, the lifetime for $^5D_0 \rightarrow {}^7F_0$ transition is $\tau \approx 8.0$ ms in $SrBPO_5$ and 9.4 ms in $BaBPO_5$. The decay curves of the $^5D_0 \rightarrow {}^7F_0$ transition in $CaBPO_5$ is not single exponential in the range of temperatures investigated. At 77 K, it can be fitted to a fast and a slow exponential process with the decay times of $\tau_1 \approx 0.9$ and $\tau_2 \approx 13.0$ ms, respectively and τ_1 decreases to ~0.3 ms at 310 K while τ_2 seems independent of temperature. The reason of this double exponential decay is not clear but may likely be caused by the energy transfer between Sm^{3+} and Sm^{2+} ions present in a certain amount in $CaBPO_5$ since the emission of $^4G_{5/2} \rightarrow {}^6H_{5/2,7/2,9/2}$ transitions of Sm^{3+} are located in the range of the absorption band of Sm^{2+} while in $BaBPO_5$, only a trace amount of Sm^{3+} was detected and hence such energy transfer process may be more ineffective than in $CaBPO_5$.

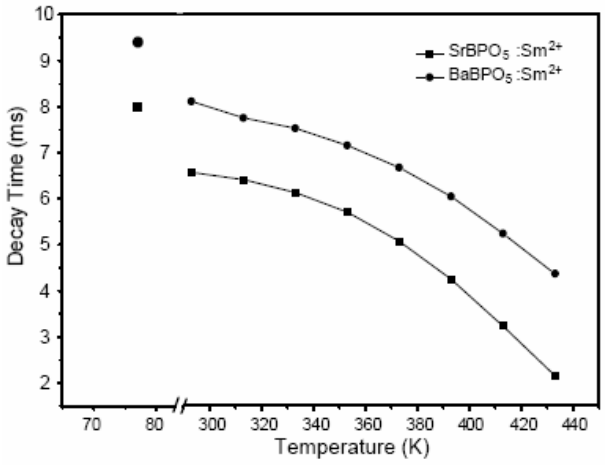

Fig. 5. The temperature dependence of the $^5D_0 \rightarrow {}^7F_0$ luminescence lifetime of Sm^{2+} in $SrBPO_5$ and $BaBPO_5$.

The radiative transition probability of the $^5D_0$–$^7F_0$ transition is an important parameter for SHB performed in this spectral line, and in general, the larger the transition probability, the higher the hole burning efficiency [27 and 28]. It was found that the transition probability of

$^5D_0$–$^7F_0$ is dependent on the energy separation between $4f^5 5d^1$ and ^5D_J levels. The smaller the energy separation, the larger the transition probability due to the mixture of the wavefunctions of $4f^5 5d^1$ and $^5D_0$ levels.

4. Conclusions

We have demonstrated that 2% samarium can be stabilized in the 2+ oxidation state in the MPO_5 ($M=Ca^{2+}$, Sr^{2+}, Ba^{2+}) host lattices when prepared in reducing atmosphere. The Sm^{2+} ion is formed exclusively for $SrBPO_5$ and $BaBPO_5$, while there is some residual Sm^{3+} present in the $CaBPO_5$ samples. We studied the luminescent properties of the $^5D_0 \rightarrow {}^7F_J$ transitions of Sm^{2+} doped in $MBPO_5$ ($M=Ca^{2+}$, Sr^{2+}, Ba^{2+}) over the temperature range from 77 to 450 K. The luminescence spectra show that there is only one crystallographic cationic site available for Sm^{2+} in all the hosts. With increasing temperature, the emission of the $^5D_0 \rightarrow {}^7F_J$ transitions of Sm^{2+} in $CaBPO_5$ decreases sharply and was completely quenched at around 350 K, while Sm^{2+} in the other two isomorphous hosts has a rather strong thermal persistence. The $^5D_1 \rightarrow {}^7F_J$ transitions of Sm^{2+} were observed in $BaBPO_5$ at 77 K and room temperature most likely because of a larger energy separation between the $^5D_1$ level and the $4f^5 5d^1$ band than in the other two hosts and its intensity increases with increasing temperature due to thermal population. In $SrBPO_5$ and $BaBPO_5$, the decay of $^5D_0 \rightarrow {}^7F_0$ transition at all temperatures investigated in this study is a single exponential process with lifetimes of $\tau \approx 8.0$ and 9.4 ms, respectively, at 77 K. The lifetimes decrease with increasing temperature. In $CaBPO_5$, the decay of the $^5D_0 \rightarrow {}^7F_0$ transition is not single exponential but can roughly be separated into a fast component with a lifetime of $\tau_1 \approx 0.9$ ms and a slow one with $\tau_2 \approx 13.0$ ms.

Acknowledgements

This work was supported by the Australian Research Council.

References

1. C. Wei, S. Huang and J. Yu *J. Lumin.* **43** (1989), p. 161.
2. D. Cho, K. Hirao, N. Soga and M. Nogami *J. Non-Cryst. Solids* **215** (1997), p. 192.
3. P. Mikhail, J. Hulliger, M. Schnieper and H. Bill *J. Mater. Chem.* **10** (2000), p. 987.
4. J. Qiu and K. Hirao *J. Mater. Sci. Lett.* **20** (2001), p. 691.
5. Z. Pei, Q. Su and J. Zhang *J. Alloys Compounds* **198** (1993), p. 51.
6. Q. Zeng, Z. Pei, Q. Su and S. Huang *Phys. Stat. Sol. (b)* **212** (1999), p. 207.
7. A. Perloff and S. Block *Acta Crystallogr.* **20** (1966), p. 274.
8. K. Machida, G. Adachi and J. Shiokawa *Acta Crystallogr. B* **36** (1980), p. 2008.
9. A.A. Vorokov and Yu.A. Pyatenko *Sov. Phys. Crystallogr.* **12** (1967), p. 214.
10. R. Kniep, G. Gozel, B. Eisenmann, C. Rohr, M. Asbrand and M. Kizilyalli *Angew. Chem. Int. Ed. Engl.* **33** (1994), p. 749.
11. Y. Shi, J. Liang, H. Zhang, Q. Liu, X. Chen, J. Yang, W. Zhuang and G. Rao *J. Solid State Chem.* **135** (1998), p. 43.
12. V.H. Bauer *Z. Anorg. Allg. Chem.* **345** (1966), p. 225.
13. H. Liang, Q. Su, Y. Tao, T. Hu and T. Liu *J. Alloys Compounds* **334** (2002), p. 293.
14. G. Blasse, A. Bril and J. De Vries *J. Inorg. Nucl. Chem.* **31** (1969), p. 568.
15. A. Karthikeyani and R. Jagannathan *J. Lumin.* **86** (2000), p. 79.
16. G. Blasse, G.J. Dirksen and A. Meijerink *Chem. Phys. Lett.* **167** (1990), p. 41.
17. A. Meijerink and G.J. Dirksen *J. Lumin.* **63** (1995), p. 189.
18. S.T. Frey, W. Dew and A. Horrocks, Jr. *Inorg. Chim. Acta* **229** (1995), p. 383.
19. V.P. Dotsenko, V.N. Radionov and A.S. Voloshinovskii *Mater. Chem. Phys.* **57** (1998), p. 134.
20. Q. Zeng, Z. Pei, S. Wang, Q. Su and S. Lu *J. Phys. Chem. Solids* **60** (1999), p. 515.
21. H.V. Lauer, Jr. and F.K. Fong *J. Chem. Phys.* **65** (1976), p. 3108.
22. C.E. Weir and R.A. Schroeder *J. Res. Nat. Bur. Stand. A* **68** (1964), p. 465.
23. A.S.M. Mahbub'ul Alam and B. Di Bartolo *J. Chem. Phys.* **47** (1967), p. 3790.
24. R.D. Shannon *Acta Crystallogr. A* **32** (1976), p. 751.
25. W.H. Fonger and C.W. Struck *J. Chem. Phys.* **69** (1978), p. 4171.
26. F. Fong, H. Lauer and C. Chilver *J. Chem. Phys.* **63** (1975), p. 366.
27. H. Song, J. Zhang, D. Gao, S. Huang and J. Yu *Opt. Commun.* **120** (1995), p. 264.
28. H. Song, T. Hayakawa and M. Nogami *J. Lumin.* **81** (1999), p. 153.